



Article

Use of Thermoregulatory Models to Evaluate Heat Stress in Industrial Environments

Irena I. Yermakova ¹, Adam W. Potter ^{2,*}, António M. Raimundo ³, Xiaojiang Xu ², Jason W. Hancock ^{2,4} and A. Virgilio M. Oliveira ^{3,5}

¹ International Scientific-Training Centre for Information Technologies and Systems, UNESCO, National Academy of Sciences, 03187 Kyiv, Ukraine; irena.yermakova@irtc.org.ua

² Thermal and Mountain Medicine Division, U.S. Army Research Institute of Environmental Medicine, 10 General Greene Avenue, Bldg 42, Natick, MA 01760, USA; xiaojiang.xu.civ@mail.mil (X.X.); jason.w.hancock5.civ@mail.mil (J.W.H.)

³ Department of Mechanical Engineering, ADAI-LAETA, University of Coimbra, Pólo II da Universidade de Coimbra, 3030-788 Coimbra, Portugal; antonio.raimundo@dem.uc.pt (A.M.R.); avfmo@isec.pt (A.V.M.O.)

⁴ Oak Ridge Institute for Science and Education (ORISE), 1299 Bethel Valley Rd., Oak Ridge, TN 37830, USA

⁵ Coimbra Polytechnic-ISEC, Rua Pedro Nunes, Quinta da Nora, 3030-199 Coimbra, Portugal

* Correspondence: adam.w.potter.civ@mail.mil

Abstract: Heat stress in many industrial workplaces imposes significant risk of injury to individuals. As a means of quantifying these risks, a comparison of four rationally developed thermoregulatory models was conducted. The health-risk prediction (HRP) model, the human thermal regulation model (HuTheReg), the SCENARIO model, and the six-cylinder thermoregulatory model (SCTM) each used the same inputs for an individual, clothing, activity rates, and environment based on previously observed conditions within the Portuguese glass industry. An analysis of model correlations was conducted for predicted temperatures (°C) of brain (T_{Brain}), skin (T_{Skin}), core body (T_{Core}), as well as sweat evaporation rate (ER ; Watts). Close agreement was observed between each model (0.81–0.98). Predicted mean \pm SD of active phases of exposure for both moderate (T_{Brain} 37.8 ± 0.25 , T_{Skin} 36.7 ± 0.49 , T_{Core} 37.8 ± 0.45 °C, and ER 207.7 ± 60.4 W) and extreme heat (T_{Brain} 39.1 ± 0.58 , T_{Skin} 38.6 ± 0.71 , T_{Core} 38.7 ± 0.65 °C, and ER 468.2 ± 80.2 W) were assessed. This analysis quantifies these heat-risk conditions and provides a platform for comparison of methods to more fully predict heat stress during exposures to hot environments.

Keywords: physiology; biophysics; thermoregulation; heat stress; glass industry



Citation: Yermakova, I.I.;

Potter, A.W.; Raimundo, A.M.;

Xu, X.; Hancock, J.W.; Oliveira,

A.V.M. Use of Thermoregulatory

Models to Evaluate Heat Stress in

Industrial Environments. *Int. J.*

Environ. Res. Public Health **2022**, *19*,

7950. [https://doi.org/10.3390/](https://doi.org/10.3390/ijerph19137950)

[ijerph19137950](https://doi.org/10.3390/ijerph19137950)

Academic Editor: Paul B.

Tchounwou

Received: 1 May 2022

Accepted: 24 June 2022

Published: 29 June 2022

Publisher's Note: MDPI stays neutral with regard to jurisdictional claims in published maps and institutional affiliations.



Copyright: © 2022 by the authors. Licensee MDPI, Basel, Switzerland. This article is an open access article distributed under the terms and conditions of the Creative Commons Attribution (CC BY) license (<https://creativecommons.org/licenses/by/4.0/>).

1. Introduction

Working conditions in the glass industry pose significant heat stress on individuals. Mitigation of heat stress in these conditions are important to ensuring a healthy workforce and to avoid risks of injury and heat disorders [1–4]. Thermal modeling provides a quantifiable and repeatable method of predicting thermal and physiological responses to various conditions and enables the development of data-driven guidance [5–8]. The present work seeks to quantify the heat-stress conditions of individual workers within the Portuguese glass industry while also comparing the predictions from four thermoregulatory models.

Thermoregulation models are powerful tools that quantitatively represent human responses to a variety of different environmental conditions (e.g., cold to hot, indoors and outdoors). A broad field of potential applications is possible, comprising predictions of the human thermal state over time, prevention of cold/hot hazards, design of mitigation plans, and assessments of physiological adjustments, among many others. Mainly due to computational restrictions, early models were designed to address specific environmental conditions (e.g., just hot or cold). However, these models have become increasingly more sophisticated to provide higher resolution details of human physiological responses, enabling the combination of complex models and the environments they may be applied to [9–13].

Typically, thermoregulation models require several features of input data, embracing at the simplest of forms (1) physical parameters of the environment, (2) human variables, (3) activity levels, and (4) clothing properties. Critical inputs of the environmental conditions include air temperature (T_a), relative humidity (RH), wind velocity (V_a), and the surrounding area temperatures (represented by radiant or mean radiant temperature (T_r , T_{mr})) and specific forms of impinging radiation (solar, etc.). The basics of the human parameters include two parts: their features (e.g., sex, stature (height), body mass, hydration status, food intake, and acclimatization status) and their activity (e.g., posture (e.g., standing, sitting) and metabolic rate (resting or active)). Clothing properties (e.g., dry and evaporative resistance, weight, textile type) are a critical element, as they represent an additional resistance layer for heat and water vapor exchange between the human body and the environment.

Validation of thermoregulation models is an important step to provide confidence in any use and interpretation of results and as a platform for making continued scientific improvements to these types of methods [14–17]. Thorough attention is usually given to this phase, while at the same time, equal importance should be given to the characterization of the environment and the measurement or estimation of the person features, physical activity, and clothing properties. If any of these approaches are neglected, the “quality” of the numerical predictions might be compromised. Conducting comparisons represents one more stage towards improvement of methods and the expansion to models capable of predicting a wide range of conditions [18–22].

This study compared the simulated outputs of four well-established, rationally designed thermoregulatory models: the health-risk prediction (HRP) model [23], the human thermal regulation model (HuTheReg) [18,24], the SCENARIO model [25–27], and the six-cylinder thermoregulatory model (SCTM) [28,29]. The use of multiple models is helpful for highlighting the range of likely outcomes while also providing quantified values to the level of heat stress and likely risk of individual workers within these conditions. While there are heat-stress guidance and standards for general workplaces and activities [30–33], extensive reviews of occupational settings [34–40], and multiple indices [21,22,41–44], this work seeks to address the specific need for quantitative guidance for these unique conditions of the glass industry.

2. Methods

2.1. Design

Each of the four thermoregulatory models (HRP, HuTheReg, SCENARIO, and SCTM) were used to simulate responses to observed heat-stress conditions within the Portuguese glass industry. Comparisons were made on the predicted brain, skin, and core body temperatures (T_{Brain} , T_{Skin} , T_{Core}) as well as the rate of heat loss from sweat evaporation (ER). These physiological variables are needed to adequately analyze heat effects on humans. Comparisons were performed between time series predictions for each measure as well as for mean \pm SD values from each phase of activity. Mean \pm SD are shown and compared between the models, and the Pearson correlation coefficients were also calculated between the model predictions during exposures.

2.1.1. Framework

The four models were used to simulate an entire workday of 8 h (480 min) in the glass industry, for which all models used the same inputs of person features, physical activity, clothing properties, and environment characteristics. These data were taken from the field survey carried out by Oliveira et al. [45], where 19 workplaces pertaining to five Portuguese glass facilities were checked. Oliveira et al. [45] assessed the heat stress using the wet bulb globe temperature (WBGT) index and the predicted heat strain (PHS) model [30,31,46,47]. These workplaces were characterized from a human thermal perspective as favorable, acceptable, critical, and very critical. However, to avoid excessive risk of heat stress, the workers only stayed in critical and very critical workplaces for limited periods of time.

Therefore, during the entire workday, each worker performs a specific “working profile” involving different workplaces.

2.1.2. Working Profiles

For practical purposes, only two glass industry working profiles were selected, more precisely, one involving workplace G12, classified by Oliveira et al. [45] as acceptable, and other involving workplace G14 (which was rated as very critical). In this study, to allow the readers an easy reference to the work of Oliveira et al. [45], the working profile involving workplace G12 is called as G_12, and the one involving workplace G14 is called as G_14. The sex of the worker was assumed as male (the most common scenario in the Portuguese glass industry), and working profiles comprising nine phases were considered (Table 1): arrival, work 1, work 2, work 1, mealtime, work 1, work 2, work 1, and departure. Workplace G_12 includes moderate heat-stress conditions, while workplace G_14 includes extreme heat-stress conditions (Table 2). The difference between the two working profiles considered occurs during the work 1 phase, where the worker is required to conduct work in moderate or extreme heat-stress conditions. Global characteristics of the surrounding environment of each workplace are shown in Table 2 for both working profiles. The overall properties of clothing worn by workers in each exposure period are shown in Table 3.

Table 1. Characteristics of the nine phases of the working day for working profiles G_12 and G_14.

Phase n°	1	2	3	4	5	6	7	8	9
Phase Name	Arrival	Work 1	Work 2	Work 1	Mealtime	Work 1	Work 2	Work 1	Departure
Exposure (min)	30	60	60	60	60	60	60	60	30
Metabolic rate (met)	1.20	2.23	2.00	2.23	1.00	2.23	2.00	2.23	1.20
Body posture	Standing	Standing	Standing	Standing	Sitting	Standing	Standing	Standing	Standing
Mass of liquids intake (kg)	0.00	0.00	0.25	0.25	0.50	0.25	0.25	0.25	0.25
Temperature of the liquids intake (°C)	0.00	0.00	20.00	20.00	20.00	20.00	20.00	20.00	20.00
Liquid specific heat (J/(kg·°C))	0.00	0.00	4.186	4.186	4.186	4.186	4.186	4.186	4.186

Table 2. Global characteristics of the surrounding environment for working profiles G_12 and G_14.

Moderate (G_12) and Extreme Heat Stress (G_14) Working Profiles							
Favorable Period (Phases 01 (Arrival), 05 (Mealtime) and 09 (Departure))							
T_a (°C)		RH (%)		V_a (m/s)		T_{mr} (°C)	
20.00		60.00		0.50		20.00	
Moderate period (phases 03 and 07 (work 2))							
25.00		50.00		0.50		25.00	
Moderate heat stress working profile (G_12)				Extreme heat stress working profile (G_14)			
Stressful periods: phases 02, 04, 06, and 08 (work 1)				Stressful periods: phases 02, 04, 06, and 08 (work 1)			
T_a (°C)	RH (%)	V_a (m/s)	T_{mr} (°C)	T_a (°C)	RH (%)	V_a (m/s)	T_{mr} (°C)
32.10	30.30	0.50	71.80	61.10	6.80	0.50	102.00

Table 3. Global clothing properties for working profiles G_12 and G_14. (Favorable (phases 01, 05, and 09), moderate (phases 03 and 07), and stressful periods (phases 02, 04, 06, and 08)).

Basic Thermal Insulation	Evaporative Resistance	Vapor Permeability Efficiency	Radiative Emissivity	Mass	Specific Heat
(clo; m ² ·°C/W)	(m ² ·kPa/W)	(N.D.)	(N.D.)	(kg)	(kJ/kg·°C)
0.603 0.093	0.700	0.478	0.906	1.3	1.0

2.2. Simulation Inputs

2.2.1. Human and Clothing Inputs

Human and clothing inputs were standardized between each of the models (Tables 1–3). The simulated worker was assumed as 1.69 m in height, a body mass of 74 kg, with an associated body surface area of 1.84 m², a resting heart rate of 65 bpm, and resting systolic pressure of 120 mm.c.Hg. Resting and active metabolic rates (*M*) were estimated following the methods of level II of accuracy of ISO 8996 [32] by adding the metabolic rates corresponding to the posture, the type of work, the body motion related to the work speed and the basal metabolic rate for each single activity. However, it is important to note that internally each of the models' approach to making these calculations differed slightly.

Clothing inputs varied in units and format for each model; however, each of them used the same fundamental values as inputs. Based on ISO 9920 [33] and on the work from Oliveira et al. [45], standardized clothing inputs of thermal insulation (clo, m²·°C/W), evaporative resistance (m²·kPa/W), radiative emissivity, mass (kg), and body surface coverage were used (Table 3). It is important note that "global values" correspond to the weighted total of the clothing on the human. That is to say, clothing parameters (e.g., thermal insulation, evaporative resistance, radiative emissivity, and mass) are functionally different values for the different body parts based on clothing coverage in that area.

2.2.2. Environmental Conditions

Oliveira et al. [45] measured the physical parameters of the environment according to ISO 7726 [48] using equipment from Brüel and Kjær and from Testo. In the case of the former, the WBGT-Heat Stress Monitor type 1219 was used to measure the natural wet bulb (T_{nw}), the 150 mm globe (T_g), and the air (T_a) temperatures. The air and globe temperatures were then used to estimate the mean radiant temperature (T_{mr}) according to the expression suggested in ISO 7726 [48,49]. For the air velocity (V_a), despite being measured (hot sphere sensor from Testo (ref. 0635 1049) connected to the data logger Testo 445 (ref. 0560 4450)), a value of 0.5 m/s was considered as representative of the type of workplaces under analysis. A humidity transducer also from Testo (ref. 0636 9741) was also connected to Testo 445. All measurements of the physical parameters were preceded by a stabilization period of 30 min.

2.2.3. Activity Phases and Exposure Times

Activity levels and phases of exposure are categorized by three periods of heat-stress potential (favorable, moderate, and stressful) and are simulated collectively over the nine phases that represent a 480 min (8 h) work day. These three types represent different environmental and activity-based characteristics, where the favorable periods represent low-intensity, low-exposure phases, shown functionally as arrival, mealtime, and departure (phases 1, 5, and 9) (Table 1). Moderate periods involve working activities in an acceptable environment and are called work 2 (phases 3 and 7). Stressful periods are referenced as work 1 (phases 2, 4, 6, and 8) and involve a high level of physical activity in a hot (G_12) or extremely hot (G_14) environment.

The exposure period of each phase is listed in Table 1. To more easily follow the path of the worker throughout the different sites that comprise the working day, greyscale

patterns in Table 1 are used in the results figures for each modeled simulation. For modeling purposes, the transition between environmental conditions occurs suddenly.

2.3. Rational Models Assessed

2.3.1. Health Risk Prediction (HRP) model

The health-risk prediction (HRP) model has a traditional structure of the human thermoregulatory system and is derived mainly from mechanistic methods, as the main predictions are calculated based on a series of equations built on a rational construct [29]. This model consists of an active part, including a regulatory center with thermal responses, and passive processes related to heat production, which are distributed through the body by conduction and convective transfer by blood and then exchanged with the environment by radiation, convection, and sweat evaporation. The model considers the human body divided into 14 parts (13 cylinders and 1 sphere) and 39 compartments (38 layers plus a blood compartment) taking into account right and left extremities.

Rational calculations of the HRP model are fairly extensive and are designed to output regional and total body temperature responses to include local skin (14 locations) and mean skin temperature, brain, blood, internal organs, muscles, and fat temperatures ($^{\circ}\text{C}$). Cardiovascular outputs from the HRP model include stroke volume (SV , mL), cardiac output (CO , L/h), and heart rate (HR , bpm). The model also allows to simulate the effect of different clothing, as it contains large database of various fabrics for composing of clothing and protective garment [50].

The HRP model has been used for modeling of human immersion in cold water [51] and in warm water [52] and validated for hot, humid conditions [20].

2.3.2. Human Thermal Regulation (HuTheReg) Model

The human thermal regulation (HuTheReg) model is a rationally designed to allow for simulations of human thermophysiological responses to a wide range of environmental conditions [8,24]. This program was implemented considering only the male sex and is composed by several modules, namely (i) male thermophysiological response, (ii) heat and water vapor transport through the clothing, (iii) heat and water exchange between the external surface of clothing (or skin) and the environment and surroundings, (iv) start and evolution of skin injuries (pain and burn), and (v) detection of specific drawbacks within the human being. Due to its interdependency, all modules run iteratively in each time step until a specific convergence criterion is reached. The main module of HuTheReg is based on work from Stolwijk [9], while more recent work has been used to expand to include additional modules for improved capabilities [11,53]. This model considers the human body divided in 22 segments (face, scalp, neck, chest, abdomen, upper back, lower back, pelvis, left shoulder, right shoulder, left arm, right arm, left forearm, right forearm, left hand, right hand, left thigh, right thigh, left leg, right leg, left foot, and right foot). Each body part is comprised of four layers (core, muscle, fat, and skin), collectively a total of 88 nodes, plus an additional node (89th) corresponding to the central blood compartment. The passive thermophysiological phenomena and the active thermoregulatory responses (shivering and vasoconstriction or sweating and vasodilatation) are simulated for each specific human body segment but considering its influence and interdependence with the global thermal state of the body. Each run can simulate up to 60 consecutive scenarios (phases), each one representing different conditions in terms of posture, orientation, activity, intake of food/drinks, clothing, and thermo-hygrometric environment characteristics. Some inputs of each phase are specified for whole human body and others for each body segment (each one considered completely nude or completed dressed).

As it is embodied in software form, the HuTheReg allows for a significant number of output calculations, both for whole body, regional elements, and for physiological calculations. The validation of the HuTheReg software was performed comparing the program's predictions with experimental results. The validation process spanned a wide-range of conditions, which included different kinds of thermo-hygrometric environments,

exposures, exercise intensities, and clothing [8,18]. A good agreement was achieved, which indicates an interesting capacity of the program to predict the thermophysiological response of the human body to a wide variety of conditions.

2.3.3. SCENARIO Thermal Model

SCENARIO thermal model is a single-cylinder, rationally based model that consists of seven compartments and is made up of five concentric cylinders that represent human core, muscle, fat, and vascular and avascular skin plus a central blood compartment and a clothing layer [25–27]. The SCENARIO model combines physiologically based variables and biophysical calculations to make time-series predictions for a given human, set of activities, and environmental exposures (i.e., scenarios). SCENARIO was developed by Kraning and Gonzalez [25–27,54] and has been recently enhanced by Tan et al. [55]. However, the model has some basis foundation from a number of key sources, namely Wyndham and Atkins [56,57], Gordon et al. [58], Stolwijk and Hardy [59], Stolwijk [9,60], Montgomery [61], Montgomery and Williams [62], Werner et al. [63–65], Gagge et al. [66–68], and Wissler [69,70]. The model requires several inputs for individual characteristics (e.g., anthropometrics, health status), environmental conditions, clothing properties (biophysics), and activity types to generate physiological predictions (metabolism, heart rate, cardiac output, stroke volume, skin, and core body temperature) over a given time course.

2.3.4. Six Cylinder Thermoregulatory Model (SCTM)

The six-cylinder thermoregulatory model (SCTM) is a rational model based on the first principles of physiology and the physical laws of heat transfer [28,29]. SCTM considers the human body subdivided into six segments representing the head, trunk, arms, legs, hands, and feet. Each segment is further divided into concentric compartments representing the core, muscle, fat, and skin. The integrated thermal signal to the thermoregulatory controller is composed of the weighted thermal input from thermal receptors at various sites distributed throughout the body. The difference between this signal and its threshold activates the thermoregulatory actions: shivering heat production, vasodilation/vasoconstriction, and sweat production. The SCTM has been validated for a broad range of conditions, including heat, cold, and water immersion [71,72]. SCTM has been used to evaluate heat strain in personal protective equipment [73] and design personal cooling systems [74]. It has been used to develop user friendly tools for operational use, probability of survival decision aid (PSDA) [75], and cold ensemble decision aid (CoWEDA) [15]. SCTM inputs include individual characteristics, intensity of activity, environmental conditions, and clothing properties (i.e., thermal resistance and evaporative resistance) for each of the six body regions. SCTM predicts physiological responses (e.g., core temperatures, skin temperatures, and sweat rates for six body regions).

2.4. Statistical Analysis

Statistical analyses were performed using MATLAB (The MathWorks, Inc., Natick, MA, USA). Descriptive statistics are presented as means \pm SD. Pearson correlation coefficients were calculated between the model predictions during exposures.

3. Results

Figure 1 shows the comparison of each models' prediction of brain (T_{Brain}), skin (T_{Skin}), and core (T_{Core}) temperatures and sweat evaporation rate (ER) over the entire work shift for the moderate working profile (G_12), while Figure 2 shows these same predictions for the stressful working profile (G_14). Additionally, Tables 4 and 5 show the mean \pm SD values for phases 2, 4, 6, and 8 for G_12 (Table 4) and G_14 (Table 5) working profiles.

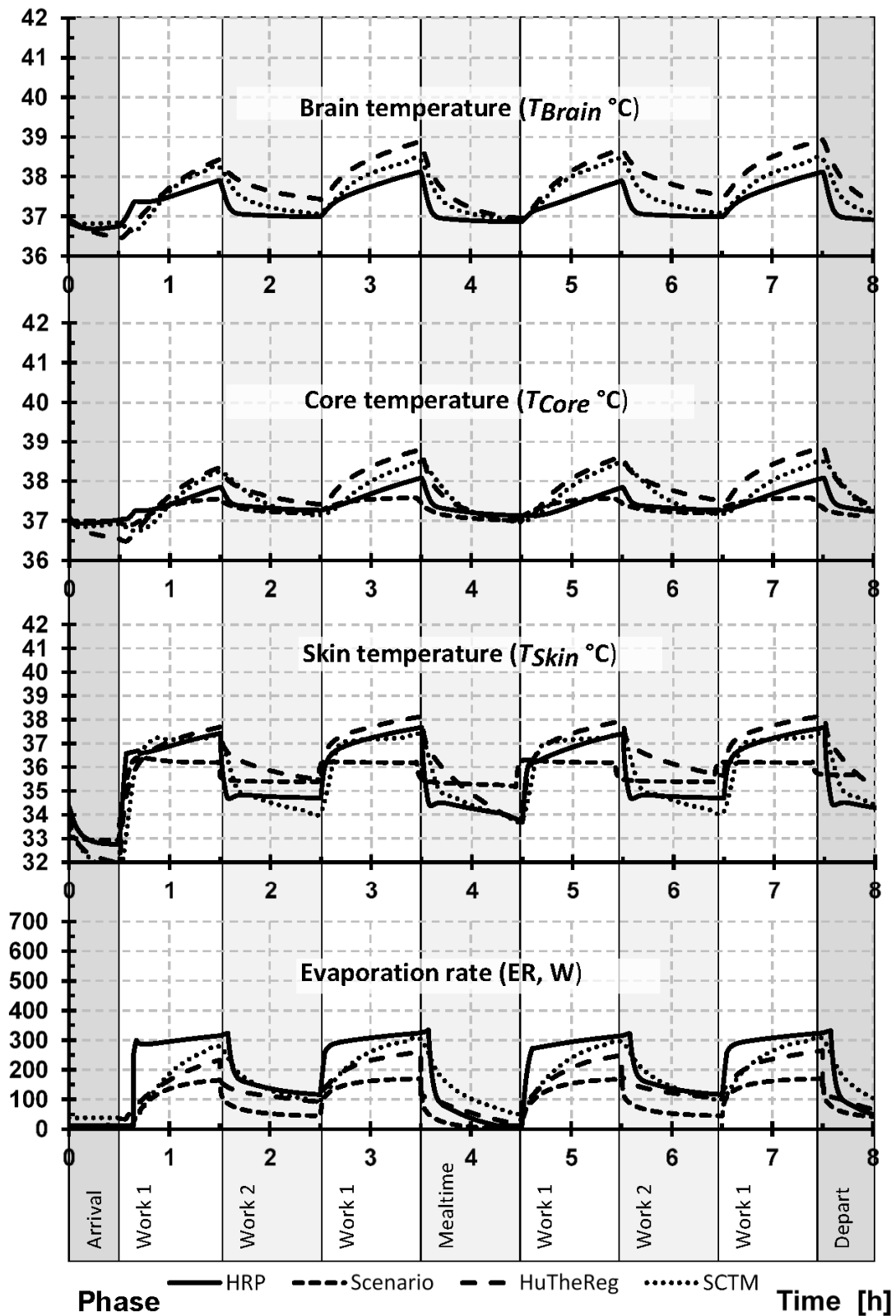


Figure 1. Predicted response pattern of brain, skin, and core body temperatures and evaporation rate during the entire work shift for moderately hot conditions (G_12). Note: HRP, health-risk prediction (HRP) model; HuTheReg, human thermal regulation model (HuTheReg); SCTM, six-cylinder thermoregulatory model.

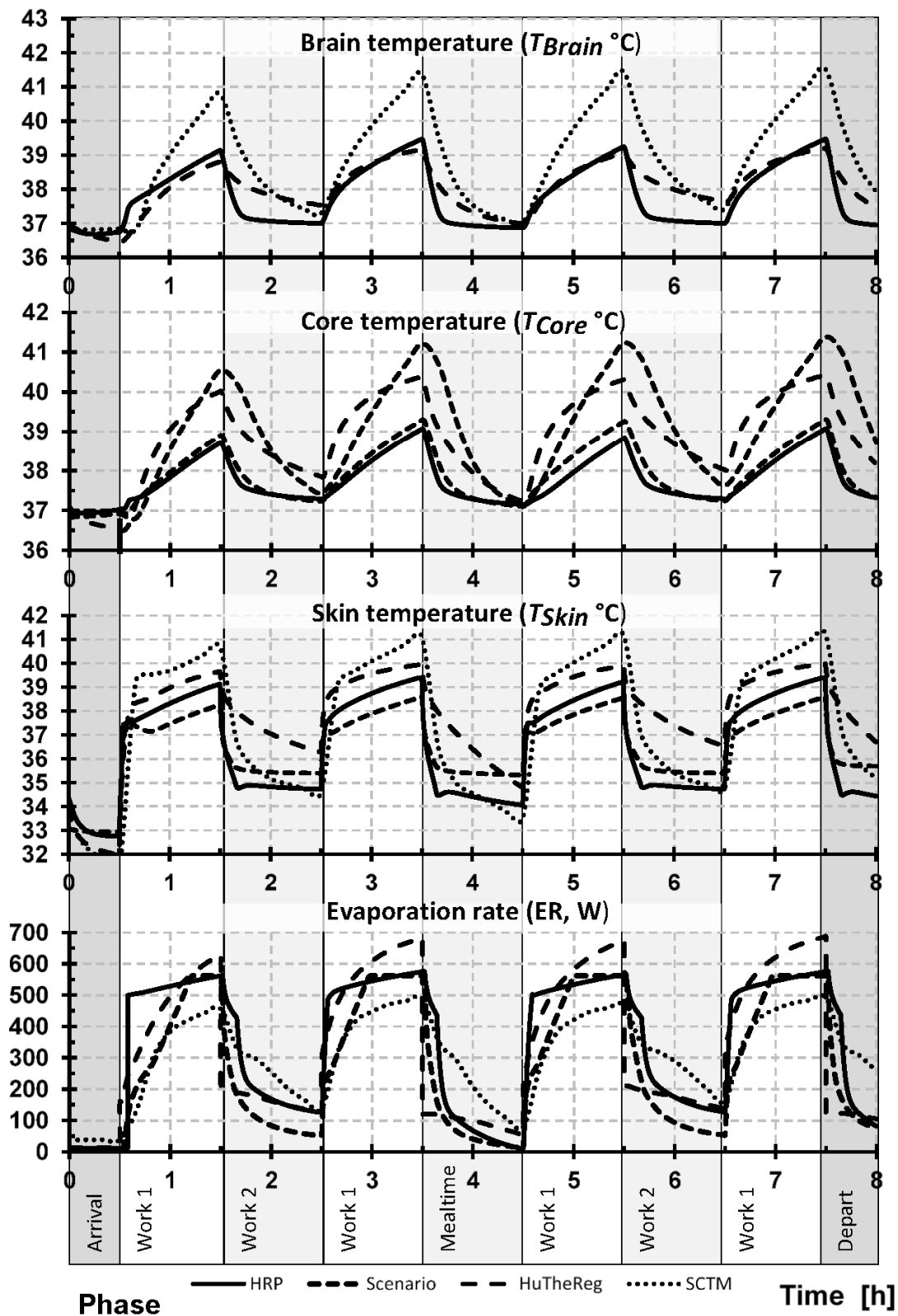


Figure 2. Predicted response pattern of brain, skin, and core body temperatures and evaporation rate during the entire work shift for extremely hot conditions (G_14). Note: HRP, health-risk prediction (HRP) model; HuTheReg, human thermal regulation model (HuTheReg); SCTM, six-cylinder thermoregulatory model.

Table 4. Mean and standard deviation values for moderate working profile G_12.

		T_{Brain} (°C)	T_{Skin} (°C)	T_{Core} (°C)	ER (W)
Phase 2	HRP	37.49 ± 0.27	36.80 ± 0.68	37.43 ± 0.23	257.42 ± 101.04
	SCENARIO	-	36.05 ± 0.65	37.28 ± 0.23	111.22 ± 56.21
	HuTheReg	37.58 ± 0.62	36.69 ± 1.15	37.51 ± 0.61	151.37 ± 61.98
	SCTM	37.49 ± 0.60	36.21 ± 1.98	37.44 ± 0.55	164.52 ± 92.14
Phase 4	HRP	37.69 ± 0.30	37.11 ± 0.50	37.67 ± 0.25	300.55 ± 29.98
	SCENARIO	-	36.18 ± 0.11	37.48 ± 0.11	153.01 ± 23.03
	HuTheReg	38.33 ± 0.43	37.57 ± 0.51	38.26 ± 0.41	218.35 ± 38.05
	SCTM	37.92 ± 0.46	36.71 ± 1.08	37.88 ± 0.47	233.73 ± 69.69
Phase 6	HRP	37.45 ± 0.27	36.74 ± 0.57	37.41 ± 0.24	280.75 ± 51.42
	SCENARIO	-	36.20 ± 0.15	37.41 ± 0.17	139.06 ± 35.88
	HuTheReg	38.00 ± 0.54	37.18 ± 0.83	37.94 ± 0.51	188.55 ± 54.26
	SCTM	37.82 ± 0.52	36.64 ± 1.17	37.77 ± 0.53	210.71 ± 81.27
Phase 8	HRP	37.69 ± 0.30	37.11 ± 0.50	37.67 ± 0.25	300.53 ± 29.99
	SCENARIO	-	36.18 ± 0.11	37.48 ± 0.11	153.03 ± 23.01
	HuTheReg	38.40 ± 0.41	37.64 ± 0.48	38.33 ± 0.40	224.05 ± 35.79
	SCTM	37.94 ± 0.45	36.72 ± 1.06	37.91 ± 0.46	236.91 ± 68.30

Table 5. Mean and standard deviation values for stressful working profile G_14.

		T_{Brain} (°C)	T_{Skin} (°C)	T_{Core} (°C)	ER (W)
Phase 2	HRP	38.24 ± 0.60	38.18 ± 0.87	37.86 ± 0.50	490.83 ± 140.63
	SCENARIO	-	37.46 ± 0.79	37.93 ± 0.61	378.26 ± 173.47
	HuTheReg	38.76 ± 1.15	38.65 ± 1.30	38.69 ± 1.14	460.59 ± 136.33
	SCTM	38.80 ± 1.47	38.71 ± 3.00	38.53 ± 1.36	311.16 ± 151.78
Phase 4	HRP	38.58 ± 0.65	38.57 ± 0.72	38.22 ± 0.53	530.14 ± 65.97
	SCENARIO	-	37.80 ± 0.58	38.39 ± 0.60	469.68 ± 128.62
	HuTheReg	39.71 ± 0.73	39.37 ± 0.63	39.64 ± 0.70	577.87 ± 97.77
	SCTM	39.62 ± 1.35	39.39 ± 2.08	39.38 ± 1.29	395.25 ± 117.27
Phase 6	HRP	38.33 ± 0.62	38.31 ± 0.75	37.96 ± 0.52	513.78 ± 85.69
	SCENARIO	-	37.76 ± 0.58	38.33 ± 0.61	460.42 ± 136.00
	HuTheReg	39.54 ± 0.92	39.18 ± 0.85	39.40 ± 0.87	545.15 ± 118.28
	SCTM	39.52 ± 1.48	39.19 ± 2.44	39.22 ± 1.42	361.09 ± 131.06
Phase 8	HRP	38.58 ± 0.65	38.58 ± 0.72	38.23 ± 0.53	530.43 ± 65.70
	SCENARIO	-	37.80 ± 0.59	38.40 ± 0.60	471.15 ± 127.73
	HuTheReg	39.80 ± 0.69	39.44 ± 0.59	39.73 ± 0.66	590.36 ± 92.78
	SCTM	39.79 ± 1.35	39.51 ± 2.05	39.56 ± 1.28	404.50 ± 109.58

Note: HRP, health-risk prediction model; HuTheReg, human thermal regulation model; SCTM, six-cylinder thermoregulatory model; T_{Brain} , brain temperature; T_{Skin} , skin temperature; T_{Core} , core body temperature; ER, sweat evaporation rate.

Exposure to both the favorable (arrival, mealtime, departure) and work 2 (moderate working periods) conditions represent the lower heat stress, while work 1 (stressful working periods) corresponds to the most significant exposure in each working condition (G_12 and G_14). As the work 1 exposures have the highest associated risk and happen four times during the day, the analyses focus mostly on these conditions. The onset of responses to

exposure to work 1 conditions can be clearly seen as a sharp increase in every parameter, followed by a decrease as the worker moves into other thermal environment (favorable or work 2 conditions). Despite the differences shown by the thermoregulation models (e.g., maximum values), the pattern in all four models is consistently the same; moreover, the mean values between each exposure are surprisingly close.

Focusing the analysis on the maximum values, it is interesting to see that despite the model, the maximum values are reached at the end of each exposure to work 1 conditions (Figures 1 and 2). Additionally, the absolute maximum is typically reached at the end of the day during the fourth exposure to work 1. This was true for the absolute predicted maximum values (T_{Brain} , T_{Skin} , T_{Core} , and ER) of each model during the moderate working profile (G_12): HRP (T_{Brain} 38.12 °C, T_{Skin} 37.67 °C, T_{Core} 38.08 °C, ER 324.32 W), HuTheReg (T_{Brain} 38.93 °C, T_{Skin} 37.76 °C, T_{Core} 38.9 °C, ER 263.55 W), SCENARIO (T_{Skin} 36.41 °C, T_{Core} 37.57 °C, ER 169.73 W), and SCTM (T_{Brain} 38.45 °C, T_{Skin} 37.30 °C, T_{Core} 38.49 °C, ER 303.97 W). This trend also held true for the absolute predicted maximum values (T_{Brain} , T_{Skin} , T_{Core} , and ER) of each model during the stressful working profile (G_14) for each model: HRP (T_{Brain} 39.08 °C, T_{Skin} 39.39 °C, T_{Core} 39.02 °C, ER 575.23 W), HuTheReg (T_{Brain} 40.52 °C, T_{Skin} 40.48 °C, T_{Core} 40.70 °C, ER 687.61 W), SCENARIO (T_{Skin} 38.59 °C, T_{Core} 39.30 °C, ER 561.80 W), and SCTM (T_{Brain} 41.53 °C, T_{Skin} 41.25 °C, T_{Core} 41.38 °C, ER 491.76 W).

Comparisons of mean values show that for each model, the four phases of exposure to work 1 are similar (Tables 4 and 5). Considering the moderate working profile (G_12) and T_{Core} , the maximum mean value is 37.51 °C (HuTheReg), and the minimum mean value is 37.28 °C (SCENARIO) in phase 2; for the remaining phases, the maximum and minimum mean values are 38.26 °C (HuTheReg) and 37.48 °C (SCENARIO) (phase 4); 37.94 °C (HuTheReg) and 37.41 °C (SCENARIO and HRP) (phase 6); and 38.33 °C (HuTheReg) and 37.48 °C (SCENARIO) (phase 8) (Table 4). For the stressful working profile (G_14), the maximum and minimum mean values are obviously higher between the T_{Core} maximum mean and the minimum mean values: 38.69 °C (HuTheReg) and 37.86 °C (HRP) (phase 2); 39.64 °C (HuTheReg) and 38.22 °C (HRP) (phase 4); 39.40 °C (HuTheReg) and 37.96 °C (HRP) (phase 6); and 39.73 °C (HuTheReg) and 38.23 °C (HRP) (phase 8) (Table 5).

Due to the extreme conditions of work 1 phases of working profile G_14, it is also important to look at the values of the sweat evaporation rate (ER); Table 5 highlights that the minimum mean value predicted by the models is 311.16 W (SCTM, phase 2), and the maximum mean value is 590.36 W (HuTheReg, phase 8). These values correspond to a significant loss of liquids (\cong 494 and 1092 g/h, respectively), thus issuing the need to pay particular attention to liquids intake throughout the day, a topic that, despite its true requirement in hot environments, is most often neglected.

Tables 6 and 7 show the calculated Pearson correlation coefficients between each of the models for both the moderate (G_12) (Table 6) and stressful working profile (G_14) (Table 7). Each of the models had a highly correlated between each other (0.8–0.9), while others were very highly correlated (0.9–1.0). The highest correlations for each working profile showed similar patterns between models, where in both G_12 and G_14, T_{Brain} was most correlated between SCTM and HuTheReg and T_{Skin} between SCTM and HRP. For G_12, the highest correlation for T_{Core} was between SCENARIO and HuTheReg (Table 6), while for G_14, the highest correlation for T_{Core} was between SCENARIO and HRP (Table 7). Correlations for ER were high in moderate conditions (G_12) between SCENARIO and HRP and between SCTM and HuTheReg (Table 6), while for the stressful working profile (G_14), they were highest between SCENARIO and HuTheReg (Table 7).

Table 6. Correlation between models predictions for moderate working profile G_12.

		HRP	SCENARIO	HuTheReg	SCTM
T_{Brain} (°C)	HRP	1.00	-	0.86	0.91
	SCENARIO	-	-	-	-
	HuTheReg	0.86	-	1.00	0.96
	SCTM	0.91	-	0.96	1.00
T_{Skin} (°C)	HRP	1.00	0.81	0.92	0.97
	SCENARIO	0.81	1.00	0.89	0.89
	HuTheReg	0.92	0.89	1.00	0.95
	SCTM	0.97	0.89	0.95	1.00
T_{Core} (°C)	HRP	1.00	0.90	0.93	0.90
	SCENARIO	0.90	1.00	0.96	0.91
	HuTheReg	0.93	0.96	1.00	0.95
	SCTM	0.90	0.91	0.95	1.00
ER (W)	HRP	1.00	0.96	0.93	0.83
	SCENARIO	0.96	1.00	0.98	0.91
	HuTheReg	0.93	0.98	1.00	0.96
	SCTM	0.83	0.91	0.96	1.00

Table 7. Correlation between models predictions for stressful working profile G_14.

		HRP	SCENARIO	HuTheReg	SCTM
T_{Brain} (°C)	HRP	1.00	-	0.87	0.90
	SCENARIO	-	-	-	-
	HuTheReg	0.87	-	1.00	0.96
	SCTM	0.90	-	0.96	1.00
T_{Skin} (°C)	HRP	1.00	0.96	0.88	0.97
	SCENARIO	0.96	1.00	0.95	0.97
	HuTheReg	0.88	0.95	1.00	0.94
	SCTM	0.97	0.97	0.94	1.00
T_{Core} (°C)	HRP	1.00	0.98	0.92	0.84
	SCENARIO	0.98	1.00	0.94	0.88
	HuTheReg	0.92	0.94	1.00	0.88
	SCTM	0.84	0.88	0.88	1.00
ER (W)	HRP	1.00	0.94	0.94	0.87
	SCENARIO	0.94	1.00	0.98	0.90
	HuTheReg	0.94	0.98	1.00	0.88
	SCTM	0.87	0.90	0.88	1.00

Note: Highlighted/bold cells indicate highest correlation for the variable of interest and condition.

4. Discussion

The present work modeled human responses to significant heat-stress exposure, which is a regular practice for the glass and ceramics industries. The extreme conditions for these workers undoubtedly impose a significant heat-stress burden; this work used four previously validated models to quantify the level of physiological strain imposed on the individuals. For the two working profiles considered (moderate G_12 and stressful G_14), clinical temperature thresholds were observed to indicate risks of heat exhaustion (best case) and of heat stroke (worst case). Using T_{Core} as a marker, in the moderate profile (G_12), most of the models (all except SCENARIO) predicted maximal temperatures indicative of potential heat exhaustion (>38 °C), while in the stressful profile (G_14), all models predicted maximal temperatures indicative of potential heat stroke (>39 °C) [76].

This study highlights some of the critically valuable information that can be gained from using thermoregulatory modeling for mitigating and planning for heat-stress con-

ditions. These analyses showed that the working conditions on the glass industry can lead the thermal status of the human body to a high hyperthermic status, which has the potential to the occurrence of harmful incidents with the workers.

There are several limitations to the current work. The use of thermoregulation models should represent a contribution to produce useful guidelines. While the mean \pm SD values could be easily calculated for the entire working day (encompassing all exposure), this analysis introduces some bias and leads to mischaracterization of the exposure. Therefore, the most critical exposures during the work shift were considered, allowing for more accurate assessment of the burden/strain and its evolution in time imposed by the thermal environment on the worker throughout the day. Additionally, given their complexity, the full details of each model were not presented, as describing them all would take away from the main goal of this work, and the number of varied and unique characteristics would make this less-than helpful for use for health and safety applications.

While some key differences between each of the models have been highlighted within the manuscript, it is important to note several others. Each of the models' input and output variables differ slightly. Some of these differences in how the models interpret responses can be seen by looking at Tables 4 and 5 in combination with Figures 1 and 2. One example can be seen in Table 4 and Figure 1, where HRP has lower deviation of temperature values but higher rates of evaporative rates compared to the other models. While it is unclear in the current work if this improves the accuracy of the model compared to the others, it shows how this higher rate of evaporation allows for more stable predicted temperatures. Additionally, the inputs for clothing properties differ between the models, as the HRP, HuTheReg, and SCTM all use regional values of clothing biophysical inputs (representing their respective model nodes), while SCENARIO uses a global (total) value to represent a weighted measure for the total body. Moreover, the algorithms used for the simulation of heat and moisture transport through clothing and between the clothing (or skin for nude elements) and the environment differs from model to model. Inputs for the environmental conditions differ slightly also, where SCENARIO, SCTM, and HuTheReg use both air temperature (T_a) and mean radiant temperature (T_{mr}) as inputs, while HRP used an operative temperature, which the mean between the T_a and T_{mr} . Additionally, the output value of T_{Core} differs in physical definition between the models, where HuTheReg considers this temperature of the intestine, and HRP, SCENARIO, and SCTM consider a rectal temperature. Similarly, T_{Brain} in HuTheReg corresponds to hypothalamus temperature and to actual brain temperature in HRP and SCTM, while SCENARIO does not predict it.

In almost all heat-stress conditions, an important part of heat imposed on the human body comes from metabolism. While each model functionally accounts for activities and makes predictions of metabolic costs in different ways, for the present work, all models used the same inputs to represent those estimated from prior work. However, it is important to note that internally each of the models' approach to making these calculations differed slightly. As metabolic heat production represents the largest influence on heat stress, it is important to accurately make these predictions (e.g., if these are incorrect, the model will be systemically impacted). For the current work, inputs for the metabolic heat production (i.e., activity rates) were performed based on methods outlined in ISO 8996 [32]. However, making more accurate and individualized methods could be used to aid in these predictions.

There are many reasons that justify differences between the models based on their origins, intended use cases, data used for development, and mathematical structures. These differences were expected along with some obvious differences in predictions. However, despite the intrinsic characteristics of each model, once validated, these models do represent powerful tools to mitigate and even to avoid heat disorders and hazards during exposures to very different thermal environments comprising both cold and hot exposures and a range of occupational (e.g., industrial, firefighting, sports) and military contexts. The present work provides one step closer to a multi-model approach to assessing these complex and different environments.

Although the comparison between the four thermoregulatory models was based only on temperatures of the brain, skin, core body, and on sweat evaporation rates, each of these models produce a wide range of other additional thermophysiological parameters. These added parameters can also be considered during the development of safety plans for working in hot environments and on ensuring prevention of workers from heat injuries and life-threatening exposures. For example, software-embodied versions of HRP, HuTheReg, and SCTM allow for output values for both the human body as a whole and for each of the body segments (i.e., core, muscle, fat, skin, and clothing temperatures) as well as physiological outputs as a whole or regionally (i.e., metabolism, heat stored and flux-rates of heat, of sweat, of water, and of work). Additionally, these models are able to provide quantitative interpretations of things such as thermal comfort or even health or injury implications (i.e., detection of heat-related disorders within the person (introversion, heat stroke, permanent brain damage, death) and skin pain, skin burn areas, and corresponding degree).

It is important for continued studies tailored to specific environments, activities, and geolocations [37,77–84] to ensure appropriate guidance can be developed to protect individuals. While it is important to note that models, guidance, and decisions aids provide significant values, ideally, direct measures from individuals should be a goal to allow for more accuracy and real-time heat-stress risk mitigation [85–88].

This work represents one outcome of a cooperation that involved researchers from very different countries and cultures. During this process, the authors worked together and shared knowledge towards a single purpose: the development of common efforts to mitigate injuries and even casualties during exposures to severe thermal environments and to improve health and safety of working conditions. In the current days, this is a statement that, in itself, despite not adding any scientific value to the present paper, the authors would like to emphasize.

5. Conclusions

This analysis shows that the working conditions of the glass industry pose significant risks of hyperthermia or, at least, have the potential to impose unsafe or harmful conditions for workers. Specifically, results quantify that the severe working conditions considered in this study lead to a very significant fluid loss (~1000 g/h), highlighting the need to pay particular attention to fluid intake throughout the working day. Moreover, if T_{Core} is used as a heat-stress marker, three of the four models predicted maximal temperatures higher than 38 °C in the moderate environment, revealing a potential heat exhaustion condition, while in the more extreme environment, all models predicted maximal temperatures higher than 39 °C, representing a serious risk of heat stroke. Pearson correlation coefficients between each of the models were highly (0.8–0.9) and very highly (0.9–1.0) related. Despite these encouraging results, the limitations of this work, being mainly related with the use of mathematical models to reproduce and simulate human behaviors, are emphasized. Finally, it is also important to stress that the full details of each model are not presented and discussed, as describing them all in detail would turn away the attention of the readers from the main goal of this work. The authors hope that the present manuscript might be helpful for use for health and safety applications, namely in hot thermal environments.

Author Contributions: Conceptualization, I.I.Y., A.W.P., A.M.R., X.X., J.W.H. and A.V.M.O.; formal analysis, A.W.P., A.M.R. and A.V.M.O.; writing—original draft preparation, review, and editing, I.I.Y., A.W.P., A.M.R., X.X., J.W.H. and A.V.M.O. All authors have read and agreed to the published version of the manuscript.

Funding: This study and analysis was funded by the U.S. Army Military Operational Medicine Research Program (MOMRP), the U.S. Army Research Institute of Environmental Medicine (USARIEM), and National Academy of Sciences for Ukraine (NAS GOV UA).

Institutional Review Board Statement: The authors have adhered to ethical principles for conducting non-human subject research. This analysis did not include any human subjects; therefore, informed consent is not applicable.

Data Availability Statement: Data from this analysis have been obtained through sharing agreements and therefore must be coordinated for use by the originators.

Acknowledgments: The authors dedicate this work to the brave men and women of Ukraine.

Conflicts of Interest: The authors declare no conflict of interest. The funders had no role in the design of the study; in the collection, analyses, or interpretation of data; in the writing of the manuscript, or in the decision to publish the results.

Disclaimer: The opinions or assertions contained herein are the private views of the authors and are not to be construed as official or as reflecting the views of the Army or the Department of Defense. 1. The investigators have adhered to the policies for protection of human subjects as prescribed in Army Regulation 70–25, and the research was conducted in adherence with the provisions of 32 CFR Part 219. 2. Citations of commercial organizations and trade names in this report do not constitute an official Department of the Army endorsement or approval of the products or services of these organizations.

Abbreviation

Abbreviation	Description (units)	Abbreviation	Description (units)
<i>Clo</i>	Clothing insulation (m ² ·°C/W)	<i>SCTM</i>	Six-cylinder thermoregulatory model
<i>CO</i>	Cardiac output (L/h)	<i>SV</i>	Stroke volume (mL)
<i>ER</i>	Evaporation rate (W)	<i>T_a</i>	Air temperature (°C)
<i>HR</i>	Heart rate (bpm)	<i>T_{Brain}</i>	Brain temperature (°C)
<i>HRP</i>	Health-risk prediction model	<i>T_{Core}</i>	Core body temperature (°C)
<i>HuTheReg</i>	Human thermal regulation Model	<i>T_g</i>	Globe temperature
<i>ISO</i>	International Organization for Standardization	<i>T_{mr}</i>	Mean radiant temperature (°C)
<i>M</i>	Metabolic rate (W)	<i>T_{nw}</i>	Natural wet bulb temperature (°C)
<i>MET</i>	Metabolic equivalent	<i>T_{Skin}</i>	Skin temperature (°C)
<i>PHS</i>	Predicted heat-strain model	<i>V_a</i>	Air velocity (m/s)
<i>RH</i>	Relative humidity (%)	<i>WBGT</i>	Wet bulb globe temperature index
<i>SCENARIO</i>	Scenario thermoregulatory model		

References

- Pogačar, T.; Žnidaršič, Z.; Bogataj, L.K.; Flouris, A.D.; Poulianiti, K.; Črepinšek, Z. Heat Waves Occurrence and Outdoor Workers' Self-assessment of Heat Stress in Slovenia and Greece. *Int. J. Environ. Res. Public Health* **2019**, *16*, 597. [[CrossRef](#)] [[PubMed](#)]
- Raimundo, A.M.; Oliveira, A.V.M.; Quintela, D.A. Thermophysiological behavior of the human body in ceramic industrial environments. In *Occupational and Environmental Safety and Health II 2020*; Arezes, P.M., Baptista, J.S., Barroso, M.P., Carneiro, P., Cordeiro, P., Costa, N., Melo, R.B., Miguel, A.S., Perestrelo, G., Eds.; Springer: Berlin/Heidelberg, Germany, 2020; pp. 189–198. [[CrossRef](#)]
- Pourmahabadian, M.; Adelhah, M.; Azam, K. Heat exposure assessment in the working environment of a glass manufacturing unit. *J. Environ. Health Sci. Eng.* **2008**, *5*, 141–147.
- Leyk, D.; Hoitz, J.; Becker, C.; Glitz, K.J.; Nestler, K.; Piekarski, C. Health risks and interventions in exertional heat stress. *Dtsch. Ärzteblatt Int.* **2019**, *116*, 537. [[CrossRef](#)] [[PubMed](#)]
- Havenith, G.; Fiala, D. Thermal indices and thermophysiological modeling for heat stress. *Compr. Physiol.* **2011**, *6*, 255–302.
- Petersson, J.; Kuklane, K.; Gao, C. Is there a need to integrate human thermal models with weather forecasts to predict thermal stress? *Int. J. Environ. Res. Public Health* **2019**, *16*, 4586. [[CrossRef](#)]
- Kingma, B.R.M.; Steenhoff, H.; Toftum, J.; Daanen, H.A.M.; Folkerts, M.A.; Gerrett, N.; Gao, C.; Kuklane, K.; Petersson, J.; Halder, A.; et al. Climapp—integrating personal factors with weather forecasts for individualised warning and guidance on thermal stress. *Int. J. Environ. Res. Public Health* **2021**, *18*, 11317. [[CrossRef](#)]
- Raimundo, A.M.; Figueiredo, A.R. Personal protective clothing and safety of firefighters near a high intensity fire front. *Fire Saf. J.* **2009**, *44*, 514–521. [[CrossRef](#)]
- Stolwijk, J.A.J. *A Mathematical Model of Physiological Temperature Regulation in Man*; NASA Contractor Report; CR-NASA: Washington, DC, USA, 1971.
- Havenith, G. Individualized model of human thermoregulation for the simulation of heat stress response. *J. Appl. Physiol.* **2001**, *90*, 1943–1954. [[CrossRef](#)]
- Fiala, D.; Lomas, K.J.; Stohrer, M. A computer model of human thermoregulation for a wide range of environmental conditions—The passive system. *J. Appl. Physiol.* **1999**, *87*, 1957–1972. [[CrossRef](#)]

12. Błażejczyk, K.; Broede, P.; Fiala, D.; Havenith, G.; Holmér, I.; Jendritzky, G.; Kampmann, B.; Kunert, A. Principles of the new Universal Thermal Climate Index (UTCI) and its application to bioclimatic research in European scale. *Misc. Geogr.* **2010**, *14*, 91–102. [[CrossRef](#)]
13. Unnikrishnan, G.; Hatwar, R.; Hornby, S.; Laxminarayan, S.; Gulati, T.; Belval, L.N.; Giersch, G.E.; Kazman, J.B.; Casa, D.J.; Reifman, J. A 3-D virtual human thermoregulatory model to predict whole-body and organ-specific heat-stress responses. *Eur. J. Appl. Physiol.* **2021**, *121*, 2543–2562. [[CrossRef](#)] [[PubMed](#)]
14. Raimundo, A.M.; Oliveira, A.V.M.; Quintela, D.A. Assessment of a human body thermoregulation software to predict the thermophysiological response of firefighters. In *Advances in Forest Fire Research 2018*; Chapter 3–Fire Management; University of Coimbra Press: Coimbra, Portugal, 2021; pp. 349–358. [[CrossRef](#)]
15. Potter, A.W.; Looney, D.P.; Santee, W.R.; Gonzalez, J.A.; Welles, A.P.; Srinivasan, S.; Castellani, M.P.; Rioux, T.P.; Hansen, E.O.; Xu, X.; et al. Validation of new method for predicting human skin temperatures during cold exposure: The Cold Weather Ensemble Decision Aid (CoWEDA). *Inform. Med. Unlocked* **2020**, *18*, 100301. [[CrossRef](#)]
16. Wang, F.; Kuklane, K.; Gao, C.; Holmér, I. Can the PHS model (ISO7933) predict reasonable thermophysiological responses while wearing protective clothing in hot environments? *Physiol. Meas.* **2010**, *32*, 239. [[CrossRef](#)] [[PubMed](#)]
17. Wang, F.; Gao, C.; Kuklane, K.; Holmér, I. Effects of various protective clothing and thermal environments on heat strain of unacclimated men: The PHS (predicted heat strain) model revisited. *Ind. Health* **2013**, *3*, 2012-0073. [[CrossRef](#)] [[PubMed](#)]
18. Berglund, L.G.; Yokota, M. *Comparison of Human Responses to Prototype and Standard Uniforms Using Three Different Human Simulation Models: HSDA, Scenario_J and Simulink2NM*; Army Research Inst of Environmental Medicine Natick MA Biophysics and Biomedical Modeling Div: Natick, MA, USA, 2005.
19. Gonzalez, R.R.; McLellan, T.M.; Withey, W.R.; Chang, S.K.; Pandolf, K.B. Heat strain models applicable for protective clothing systems: Comparison of core temperature response. *J. Appl. Physiol.* **1997**, *83*, 1017–1032. [[CrossRef](#)]
20. Potter, A.W.; Yermakova, I.I.; Hunt, A.P.; Hancock, J.W.; Oliveira, A.V.M.; Looney, D.P.; Montgomery, L.D. Comparison of two mathematical models for predicted human thermal responses to hot and humid environments. *J. Therm. Biol.* **2021**, *97*, 10. [[CrossRef](#)]
21. Zare, S.; Shirvan, H.E.; Hemmatjo, R.; Nadri, F.; Jahani, Y.; Jamshidzadeh, K.; Paydar, P. A comparison of the correlation between heat stress indices (UTCI, WBGT, WBGT, TSI) and physiological parameters of workers in Iran. *Weather. Clim. Extrem.* **2019**, *26*, 100213. [[CrossRef](#)]
22. de Freitas, C.R.; Grigorieva, E.A. A comparison and appraisal of a comprehensive range of human thermal climate indices. *Int. J. Biometeorol.* **2017**, *61*, 487–512. [[CrossRef](#)]
23. Yermakova, I.; Nikolaienko, A.; Grigorian, A. Dynamic model for evaluation of risk factors during work in hot environment. *J. Phys. Sci. Appl.* **2013**, *3*, 238–243.
24. Raimundo, A.M.; Quintela, D.A.; Gaspar, A.R.; Oliveira, A.V.M. Development and validation of a computer program for simulation of the human body thermophysiological response. In *Proceedings of the 2012 IEEE 2nd Portuguese Meeting in Bioengineering (ENBENG)*, Coimbra, Portugal, 23–25 February 2012.
25. Kraning, K.K.; Gonzalez, R.R. *SCENARIO: A Military/Industrial Heat Strain Model Modified to Account for Effects of Aerobic Fitness and Progressive Dehydration*; April. Report No.: TN97-1; Army Research Inst of Environmental Medicine Natick MA: Natick, MA, USA, 1997.
26. Kraning, K.K.; Gonzalez, R.R. A mechanistic computer simulation of human work in heat that accounts for physical and physiological effects of clothing, aerobic fitness, and progressive dehydration. *J. Therm. Biol.* **1997**, *22*, 331–342. [[CrossRef](#)]
27. Gonzalez, R.R. *SCENARIO revisited: Comparisons of operational and rational models in predicting human responses to the environment*. *J. Therm. Biol.* **2004**, *29*, 515–527. [[CrossRef](#)]
28. Xu, X.; Werner, J. A dynamic model of the human/clothing/environment-system. *Appl. Hum. Sci.* **1997**, *16*, 61–75. [[CrossRef](#)] [[PubMed](#)]
29. Xu, X.; Tikuisis, P.; Gonzalez, R.; Giesbrecht, G. Thermoregulatory model for prediction of long-term cold exposure. *Comput. Biol. Med.* **2005**, *35*, 287–298. [[CrossRef](#)] [[PubMed](#)]
30. *ISO 7243; Hot Environments-Estimation of the Heat Stress on Working Man, Based on the WBGT Index (Wet Bulb Globe Temperature)*. 3rd ed. ISO: Geneva, Switzerland, 2017.
31. *ISO 7933; Ergonomics of the Thermal Environment-Analytical Determination and Interpretation of Heat Stress Using Calculation of the Predicted Heat Strain*. 2nd ed. ISO: Geneva, Switzerland, 2014.
32. *ISO 8996; Ergonomics of the Thermal Environment-Determination of Metabolic Rate*. 2nd ed. ISO: Geneva, Switzerland, 2004.
33. *ISO 9920; Ergonomics of the Thermal Environment-Estimation of the Thermal Insulation and Water Vapour Resistance of a Clothing Ensemble*. 2nd ed. ISO: Geneva, Switzerland, 2007.
34. Gao, C.; Kuklane, K.; Östergren, P.; Kjellstrom, T. Occupational heat stress assessment and protective strategies in the context of climate change. *Int. J. Biometeorol.* **2018**, *62*, 359–371. [[CrossRef](#)]
35. Tjaša Pogačar, T.; Casanueva, A.; Kozjek, K.; Ciuha, U.; Mekjavić, I.B.; Bogataj, L.K.; Zalika Črepinšek, Z. The effect of hot days on occupational heat stress in the manufacturing industry: Implications for workers' well-being and productivity. *Int. J. Biometeorol.* **2018**, *62*, 1251–1264. [[CrossRef](#)]

36. Afshari, D.; Moradi, S.; Angali, K.A.; Shirali, G. Estimation of Heat Stress and Maximum Acceptable Work Time Based on Physiological and Environmental Response in Hot-Dry Climate: A Case Study in Traditional Bakers. *Int. J. Occup. Environ. Med.* **2019**, *10*, 194–202. [[CrossRef](#)]
37. Lundgren Kownacki, K.; Gao, C.; Kuklane, K.; Wierzbicka, A. Heat Stress in Indoor Environments of Scandinavian Urban Areas: A Literature Review. *Int. J. Environ. Res. Public Health* **2019**, *16*, 560. [[CrossRef](#)]
38. Ahmed, H.O.; Bindekhain, J.A.; Alshuweih, M.I.; Yunis, M.A.; Matar, N.R. Assessment of thermal exposure level among construction workers in UAE using WBGT, HSI and TWL indices. *Ind. Health* **2020**, *58*, 170–181. [[CrossRef](#)]
39. Foster, J.; Smallcombe, J.W.; Hodder, S.; Jay, O.; Flouris, A.D.; Lars Nybo, L.; Havenith, G. An advanced empirical model for quantifying the impact of heat and climate change on human physical work capacity. *Int. J. Biometeorol.* **2021**, *65*, 1215–1229. [[CrossRef](#)]
40. Ioannou, L.G.; Foster, J.; Morris, N.B.; Piil, J.F.; Havenith, G.; Mekjavic, I.B.; Kenny, G.P.; Nybo, L.; Flouris, A.D. Occupational heat strain in outdoor workers: A comprehensive review and meta-analysis. *Temperature* **2022**, *9*, 67–102. [[CrossRef](#)]
41. Binarti, F.; Koerniawan, M.D.; Triyadi, S.; Utami, S.S.; Matzarakis, A. A review of outdoor thermal comfort indices and neutral ranges for hot-humid regions. *Urban Clim.* **2020**, *31*, 100531. [[CrossRef](#)]
42. Yasmeen, S.; Liu, H. September. Evaluation of thermal comfort and heat stress indices in different countries and regions—A Review. In *IOP Conference Series: Materials Science and Engineering*; IOP Publishing: Bristol, UK, 2019; Volume 609, p. 052037.
43. Matzarakis, A. Curiosities about thermal indices estimation and application. *Atmosphere* **2021**, *12*, 721. [[CrossRef](#)]
44. Staiger, H.; Laschewski, G.; Matzarakis, A. Selection of appropriate thermal indices for applications in human biometeorological studies. *Atmosphere* **2021**, *10*, 18. [[CrossRef](#)]
45. Oliveira, A.V.M.; Gaspar, A.R.; Raimundo, A.M.; Quintela, D.A. Assessment of Thermal Environments: Working Conditions in the Portuguese Glass Industry. *Ind. Health* **2018**, *56*, 62–77. [[CrossRef](#)] [[PubMed](#)]
46. Malchaire, J.B.; Piette, A.; Kampmann, B.; Mehnert, P.; Gebhardt, H.J.; Havenith, G.; Den Hartog, E.; Holmer, I.; Parsons, K.; Alfano, G.; et al. Development and validation of the predicted heat strain model. *Ann. Occup. Hyg.* **2001**, *45*, 123–135. [[CrossRef](#)] [[PubMed](#)]
47. Malchaire, J.B. Occupational heat stress assessment by the Predicted Heat Strain model. *Ind. Health* **2006**, *44*, 380–387. [[CrossRef](#)]
48. *ISO 7726; Ergonomics of the Thermal Environment-Instruments for Measuring Physical Quantities*. 2nd ed. ISO: Geneva, Switzerland, 1998.
49. Oliveira, A.V.M.; Raimundo, A.M.; Gaspar, A.R.; Quintela, D.A. Globe Temperature and its Measurement: Requirements and Limitations. *Ann. Work. Expo. Health* **2019**, *63*, 743–758. [[CrossRef](#)]
50. Troynikov, O.; Nawaz, N.; Yermakova, I. Materials and engineering design for human performance and protection in extreme hot conditions. In *Advances in Engineering Materials; product and systems design*; Trans Tech Publications Ltd.: Bäch, Switzerland, 2013; Volume 633, pp. 169–180. [[CrossRef](#)]
51. Yermakova, I.; Nikolaienko, A.; Solopchuk, Y.; Regan, M. Modelling of human cooling in cold water: Effect of immersion level. *Extrem. Physiol. Med.* **2015**, *4*, A132. [[CrossRef](#)]
52. Yermakova, I.; Montgomery, L.; Nikolaienko, A.; Bondarenko, Y.; Ivanushkina, N. Modeling Prediction of Human Thermal Responses in Warm Water. *Med. Inform. Eng.* **2021**, *1*, 51–60. [[CrossRef](#)]
53. Tanabe, S.; Kobayashi, K.; Nakano, J.; Ozeki, Y.; Konishi, M. Evaluation of thermal comfort using combined multi-node thermoregulation (65MN) and radiation models and computational fluid dynamics (CFD). *Energy Build* **2002**, *34*, 637–646. [[CrossRef](#)]
54. Kraning, K.K. *A Computer Simulation for Predicting the Time Course of Thermal and Cardiovascular Responses to Various Combinations of Heat Stress, Clothing and Exercise*; Report No.: T13-91; Army Research Inst of Environmental Medicine Natick MA: Natick, MA, USA, 1991.
55. Tan, A.P.; Cheong, C.H.; Lee, T.; Seng, K.Y.; Teo, C.J. Computer modelling of heat strain responses of exercising personnel in tropical climate. *Comput. Biol. Med.* **2021**, *134*, 104530. [[CrossRef](#)] [[PubMed](#)]
56. Wyndham, C.; Atkins, A. A physiological scheme and mathematical model of temperature regulation in man. *Pflügers Archiv.* **2021**, *303*, 14–30. [[CrossRef](#)] [[PubMed](#)]
57. Atkins, A.; Wyndham, C. A study of temperature regulation in the human body with the aid of an analogue computer. *Pflügers Archiv.* **1969**, *307*, 104–119. [[CrossRef](#)]
58. Gordon, R.G.; Roemer, R.B.; Horvath, S.M. A mathematical model of the human temperature regulatory system-transient cold exposure response. *IEEE Trans. Biomed. Eng.* **1976**, *23*, 434–444. [[CrossRef](#)] [[PubMed](#)]
59. Stolwijk, J.; Hardy, J. Temperature regulation in man—A theoretical study. *Pflügers Archiv* **1966**, *291*, 129–162. [[CrossRef](#)] [[PubMed](#)]
60. Stolwijk, J.A. Mathematical models of thermal regulation. *Ann. N. Y. Acad. Sci.* **1980**, *335*, 98–106. [[CrossRef](#)]
61. Montgomery, L.D. A model of heat transfer in immersed man. *Ann. Biomed. Eng.* **1974**, *2*, 19–46. [[CrossRef](#)]
62. Montgomery, L.D.; Williams, B.A. Effect of ambient temperature on the thermal profile of the human forearm, hand, and fingers. *Ann. Biomed. Eng.* **1976**, *4*, 209–219. [[CrossRef](#)]
63. Werner, J. Thermoregulatory models: Resent research, current applications and future development. *Scand. J. Work Environ. Health* **1989**, *15*, 34–46.
64. Werner, J.; Buse, M.; Foegen, A. Lumped versus distributed thermoregulatory control: Results from a three-dimensional dynamic model. *Biol. Cybern.* **1989**, *62*, 63–73. [[CrossRef](#)]

65. Werner, J.; Webb, P. A six-cylinder model of for general use on human thermoregulation personal computers. *Ann. Physiol. Anthropol.* **1993**, *12*, 123–134. [[CrossRef](#)] [[PubMed](#)]
66. Gagge, A.P.; Stolwijk, J.; Hardy, J. Comfort and thermal sensations and associated physiological responses at various ambient temperatures. *Environ. Res.* **1967**, *1*, 1–20. [[CrossRef](#)]
67. Gagge, A.; Stolwijk, J.; Nishi, Y. An effective temperature scale based on a simple model of human physiological regulatory response. In *Memoirs of the Faculty of Engineering*; Hokkaido University: Freienbach, Switzerland, 1972; Volume 13, pp. 21–36.
68. Gagge, A.P.; Stolwijk, J.A.J.; Nishi, Y. An effective temperature scale based on a simple model of human physiological regulatory response. *ASHRAE Trans.* **1971**, *77*, 247–262.
69. Wissler, E.H. A mathematical model of the human thermal system. *Bull. Math. Biophys.* **1964**, *26*, 147–166. [[CrossRef](#)] [[PubMed](#)]
70. Wissler, E.H. Comparison of computed results obtained from two mathematical models: A simple 14-node model and a complex 250-node model. *J. De Physiol.* **1971**, *63*, 455.
71. Xu, X.; Castellani, J.W.; Santee, W.; Kolka, M. Thermal responses for men with different fat compositions during immersion in cold water at two depths: Prediction versus observation. *Eur. J. Appl. Physiol.* **2007**, *100*, 79–88. [[CrossRef](#)]
72. Xu, X.; Turner, C.A.; Santee, W.R. Survival time prediction in marine environments. *J. Therm. Biol.* **2011**, *36*, 340–345. [[CrossRef](#)]
73. Xu, X.; Gonzalez, J.A.; Santee, W.R.; Blanchard, L.A.; Hoyt, R.W. Heat strain imposed by personal protective ensembles: Quantitative analysis using a thermoregulation model. *Int. J. Biometeorol.* **2016**, *60*, 1065. [[CrossRef](#)]
74. Xu, X.; Berglund, L.G.; Chevront, S.N.; Endrusick, T.L.; Kolka, M.A. Model of human thermoregulation for intermittent regional cooling. *Aviat. Space Environ. Med.* **2004**, *75*, 1065–1069.
75. Xu, X.; Amin, M.; Santee, W.R. *Probability of Survival Decision Aid (PSDA)*; Report No.: USARIEM T08/05, ADA478415; US Army Research Institute of Environmental Medicine: Natick MA, USA, 2008.
76. Bouchama, A.; Knochel, J.P. Heat stroke. *N. Engl. J. Med.* **2002**, *346*, 1978–1988. [[CrossRef](#)]
77. Venugopal, V.; Chinnadurai, J.S.; Lucas, R.A.; Kjellstrom, T. Occupational heat stress profiles in selected workplaces in India. *Int. J. Environ. Res. Public Health* **1988**, *13*, 89. [[CrossRef](#)] [[PubMed](#)]
78. Ioannou, L.G.; Mantzios, K.; Tsoutsoubi, L.; Nintou, E.; Vliora, M.; Gkiata, P.; Dallas, C.N.; Gkikas, G.; Agaliotis, G.; Sfakianakis, K.; et al. Occupational heat stress: Multi-country observations and interventions. *Int. J. Environ. Res. Public Health* **2016**, *18*, 6303. [[CrossRef](#)] [[PubMed](#)]
79. Tawatsupa, B.; Yiengprugsawan, V.; Kjellstrom, T.; Berecki-Gisolf, J.; Seubsman, S.A.; Sleigh, A. Association between heat stress and occupational injury among Thai workers: Findings of the Thai Cohort Study. *Ind. Health* **2019**, *51*, 34–46. [[CrossRef](#)] [[PubMed](#)]
80. Wagoner, R.S.; López-Gálvez, N.I.; de Zapien, J.G.; Griffin, S.C.; Canales, R.A.; Beamer, P.I. An occupational heat stress and hydration assessment of agricultural workers in North Mexico. *Int. J. Environ. Res. Public Health* **2013**, *17*, 2102. [[CrossRef](#)]
81. Jay, O.; Brotherhood, J.R. Occupational heat stress in Australian workplaces. *Temperature* **2020**, *3*, 394–411. [[CrossRef](#)]
82. Heidari, H.; Golbabaee, F.; Shamsipour, A.; Rahimi Forushani, A.; Gaeni, A. Outdoor occupational environments and heat stress in Iran. *J. Environ. Health Sci. Eng.* **2016**, *13*, 48. [[CrossRef](#)]
83. Messeri, A.; Morabito, M.; Bonafede, M.; Bugani, M.; Levi, M.; Baldasseroni, A.; Binazzi, A.; Gozzini, B.; Orlandini, S.; Nybo, L.; et al. Heat stress perception among native and migrant workers in Italian industries—Case studies from the construction and agricultural sectors. *Int. J. Environ. Res. Public Health* **2015**, *16*, 1090. [[CrossRef](#)]
84. Acharya, P.; Boggess, B.; Zhang, K. Assessing heat stress and health among construction workers in a changing climate: A review. *Int. J. Environ. Res. Public Health* **2019**, *15*, 247. [[CrossRef](#)]
85. Friedl, K.E.; Buller, M.J.; Tharion, W.J.; Potter, A.W.; Manglapus, G.L.; Hoyt, R.W. *Real Time Physiological Status Monitoring (RT-PSM): Accomplishments, Requirements, and Research Roadmap*; Technical Note, TN16-02; U.S. Army Research Institute of Environmental Medicine: Natick, MA, USA, 2016.
86. Pancardo, P.; Acosta, F.D.; Hernández-Nolasco, J.A.; Wister, M.A.; López-de-Ipiña, D. Real-time personalized monitoring to estimate occupational heat stress in ambient assisted working. *Sensors* **2015**, *15*, 16956–16980. [[CrossRef](#)]
87. Egbert, J.; Krenz, J.; Sampson, P.D.; Jung, J.; Calkins, M.; Zhang, K.; Palmáñez, P.; Faestel, P.; Spector, J.T. Accuracy of an estimated core temperature algorithm for agricultural workers. *Arch. Environ. Occup. Health* **2015**, 1–10. [[CrossRef](#)]
88. Sulzer, M.; Christen, A.; Matzarakis, A. A Low-Cost Sensor Network for Real-Time Thermal Stress Monitoring and Communication in Occupational Contexts. *Sensors* **2022**, *22*, 1828. [[CrossRef](#)] [[PubMed](#)]